RSC Advances

PAPER

View Article Online
View Journal | View Issue

Cite this: *RSC Adv.*, 2025, **15**, 6100

Experimental heat capacity of highly stable diamond/thermal oil nano-suspensions

Anas Ahmed,[a] Suhaib Umer Ilyas, *[b] Nawal Noshad,[c] Mustafa Alsaady,[b] Aymn Abdulrahman,[b] Abdullah Bin Mahfouz[b] and Abulhassan Ali[d]

Received 23rd November 2024
Accepted 12th February 2025

DOI: 10.1039/d4ra08312a

rsc.li/rsc-advances

The addition of nanoparticles into conventional fluids changes their thermophysical properties, such as thermal conductivity, viscosity, density, and specific heat capacity (SHC). While different nanofluids' thermal conductivity and viscosity are studied extensively, only a few experimental studies are subjected to SHC properties. It is important to investigate the SHC of nanofluids to understand their thermal aspects, particularly where the literature shows ambiguous results for the SHC of nanofluids. This study measures the SHC of diamond-based thermal oil nanofluids using differential scanning calorimeter (DSC) at varying nanoparticle concentrations of 0.25, 0.5, 0.75, and 1 wt% and a temperature range of 35–80 °C. The SHC of these nanofluids increased with temperature and decreased with an increase in nanoparticle concentration with a maximum SHC decrement of 8.25% at the highest 1 wt% concentration. The classical models are proved to underpredict the SHC of diamond-thermal oil nanofluids, as many nano-scale phenomena are not considered in these models. Therefore, a new multivariable correlation is also proposed for predicting the SHC of diamond-thermal oil nanofluids, exhibiting a good agreement with the experimental data with an R^2 of 96.35%.

Introduction

Pertinent issues like climate change and global warming make it increasingly significant to take into consideration inefficient thermal management and thus the excessive loss of energy into the atmosphere. In order to contribute to the mitigation of climate change and its effects, it is essential to limit these emissions by assessing the heat transfer performance of heat exchange and recovery systems, which are found in most domestic and industrial applications.[1,2] Using heat transfer fluids with enhanced thermal properties is a promising way to increase the energy efficiency of these systems.[3–5]

Nanofluids are colloidal suspensions in which nanoparticles of size 10–100 nm are dispersed in different base fluids (water, ethylene glycol, thermal oil *etc.*). Metals, metal oxides, carbon allotropes and other compounds may be used as nanoparticle additives to base fluids so as to improve their heat transfer characteristics by altering thermophysical properties like thermal conductivity, viscosity, specific heat, density *etc.* While thermal conductivity[6–8] and viscosity[9–11] have been studied extensively on account of investigating thermal applications and flow behavior, comparatively fewer experimental studies are available on the specific heat of nanofluids.[12]

Specific heat capacity (SHC) is an essential thermophysical property in several aspects concerning thermal energy storage and fluid flow management.[13,14] Specific heat can be used to express nanofluid performance in thermal installations by evaluating energy balances of heat exchangers, calculations of Prandtl number, and important properties such as thermal conductivity, thermal diffusivity, *etc.*[14,15] The addition of nanoparticles into base fluids changes the SHC of the nanofluids.[16] The evolution of nanomaterial technology leaves room for researchers to study the heat capacity of different colloidal suspensions at varying temperatures and concentrations. Among several methods, such as the transient heating wire method,[17] and the temperature history method,[18] the most common means of specific heat measurement is the differential scanning calorimeter (DSC). DSC measures the heat flux of the sample under a specified heat regime as a function of temperature.[19]

Several researchers have utilized DSC for the measurement of nanofluids' SHC (given in Table 1). Akilu *et al.*[14] measured the SHC of SiO_2 nanoparticles in glycerol, EG, and glycerol + EG mixture (60 : 40) using DSC at different volume concentrations (1–4%) and temperatures (25 °C and 50 °C). These nanofluids had a lower SHC than their corresponding base fluids, which decreased further with an increase in nanoparticle concentration but increased with temperature. Moreover, SHC values

[a]*Industrial and Systems Engineering Department, University of Jeddah, Jeddah 23890, Kingdom of Saudi Arabia*

[b]*Chemical Engineering Department, University of Jeddah, Jeddah 23890, Kingdom of Saudi Arabia. E-mail: suilyas@uj.edu.sa*

[c]*School of Chemical and Materials Engineering, National University of Sciences and Technology, Islamabad 44000, Pakistan*

[d]*School of Chemistry and Chemical Engineering, Queen's University Belfast, University Rd, Belfast BT7 1NN, UK*

Table 1 Studies on SHC measurement of nanofluids by DSC

References	Nanofluids	Temperatures	DSC equipment	SHC results
Adun *et al.*[24]	Fe_3O_4–Al_2O_3–ZnO/water	25–65 °C	Mettler Toldeo 823 DSC	The highest SHC increment of 14.6% was observed at 1.25% vol. concentration and 25 °C compared to base fluid for 1 : 2 : 1 nanoparticle ratio
Hosseinghorbani *et al.*[25]	Functionalized graphene oxide (GO)/ ionic liquid	15–65 °C	MDSC 2910, TA Instrument Inc., New Castle, DE	SHC of ionic nanofluids with 0.5, 1.0 and 2 wt% of GO nanoparticles increased by up to 27%, 35% and 42%, respectively
Said *et al.*[26]	rGO-Co_3O_4/water	25–60 °C	DSC 2920 modulated, TA Instruments	Maximum decrease in SHC compared to base fluid was 0.17%, at 60 °C for 0.2 wt% concentration
Wole-Osho *et al.*[27]	Al_2O_3–ZnO/water	25–65 °C	Mettler Toldeo 823 DSC	Maximum SHC reduction compared to base fluid was 30.12% at 1.67% vol. concentration and 25 °C for 2 : 1 nanoparticle mixture ratio
Yarmand *et al.*[28]	Graphene nanoplatelets (GNP)-Pt/water	5–100 °C	DSC 8000, Perkin Elmer, USA	SHC of nanofluid was 1.77% and 6.26% lower than base fluid for 0.02 and 0.1 wt% of nanoparticles respectively at 45 °C
Akilu *et al.*[29]	SiO_2–CuO/C/glycerol + ethylene glycol	303.15–353.15 K	Automated sampler DSC Q2000, TA Instruments, USA	The most noticeable SHC decrement was 21.1% for 2% volume concentration of SiO_2–CuO/C at 303.15 K
Paul *et al.*[30]	Al_2O_3/ionic liquid	25–345 °C	DSC Q2000, TA Instruments Inc	SHC of ionic liquid nanofluids was increased by 49% for nanoparticle loading of 0.9 vol%
Ijam *et al.*[31]	Graphene oxide nanosheets (GON)/ deionized water + ethylene glycol (60 : 40)	20–60 °C	DSC 4000, Perkin Elmer	The SHC of the nanofluid increased by 3.59–5.28% with a weight fraction of 0.05% and decreased by 9.05–8.215% with weight fraction of 0.10%
Gómez-Villarejo *et al.*[32]	BN nanotubes/Triton X-100 + water	20–70 °C	DSC 214 Polyma, Netzsch	The isobaric specific heat increased by 8.3% and 8.0% with respect to water and the base fluid at 70 °C
Vallejo *et al.*[33]	GNP/ethylene glycol + water (50 : 50)	293.15–333.15 K	Q2000 DSC, TA Instruments, New Castle, USA	Up to 0.63% SHC decrements were obtained from 0–1 wt% of nanoadditive
Marcos *et al.*[34]	Carbon black (CB)/ polyethylene glycol (PEG200)	233.15–353.15 K	DSC Q2000, TA Instruments, New Castle, DE, USA	The polyvinlpyrrolidone (PVP) surfactant addition to PEG200 gives isobaric SHC decrement up to 6% whereas the dispersion of CB to PVP + PEG200 results in SHC reductions up to 3.2%
Vallejo *et al.*[35]	GNP/propylene glycol + water (30 : 70)	293.15–323.15 K	DSC Q2000, TA Instruments, New Castel, USA	A decreasing trend of SHC was observed with nanoadditive loading. The increases in SHC reach up to 1.8% in the studied temperature range
Chen *et al.*[36]	SiC/ionic liquid	0–80 °C	DSC 823, Mettler Toledo, Switzerland	SHC enhancements of 0.9%, 3.2% and 5% were observed in comparison to base ionic liquid for 0.01, 0.03 and 0.06 wt% SiC, respectively at 25 °C
Żyła *et al.*[37]	Nanodiamond/ethylene glycol	298.15 K	DSC Q2000, TA Instruments, New Castle, USA	SHC decreasing of up to 7.3% were achieved for the highest analyzed concentration compared to ethylene glycol base fluid

agreed well with the thermal equilibrium model. Gamal *et al.*[20] studied the SHC of MgO and ZnO nanoparticles in water and EG + water mixtures with volume concentrations ranging from 0.25 to 1%, temperatures from 40 to 120 °C, and ratio of ethylene glycol in the EG + water mixture from 0 to 60%. Similar results were obtained where SHC decreased with increase in particle concentration (and EG concentration) and increased with temperature. In another study,[21] SHC of different ionic

nanofluids was studied over the temperature range of 80–370 K and was found to be an additive quantity of the SHC of its components.

Cabaleiro *et al.*[15] used a quasi-isothermal temperature modulated differential scanning calorimeter (MDSC) to measure SHC of metal oxide nanofluids, *i.e.*, MgO, ZnO, and ZrO_2 nanoparticles in EG, and ZnO and ZrO_2 nanoparticles in EG + water mixtures (50 : 50 in volume) for up to 15% mass concentrations and in the temperature range 243.15–473.15 K. SHC increased with temperature (45% for EG-based nanofluids and 24% for EG + water-based nanofluids) and decreased as the nanoparticle concentration increased (9% for MgO/EG and 12% for both ZnO and ZrO_2 nanofluids). Another study[22] investigated the SHC and viscosity of MgO/polyethylene glycol 400. SHC results revealed a decrease of 5.89–22.4% with the addition of nanoparticles. A larger decrease was observed for high concentrations. However, there was a 4.9–17.1% enhancement of SHC (depending on concentration) with temperature. In a study[23] contradictory to either increase or decrease of SHC, the addition of carbon nanotubes into ionic liquids had little (not greater than 3.1%) or no significant influence on the SHC of the 43 ionic nanofluid systems that were examined.

While the SHC of some of these nanofluids are found to be lower than their base fluids (which can be advantageous where quick temperature changes are required[5]), cases of SHC enhancement can be particularly useful in applications that involve thermal storage. An increase of SHC by the addition of nanoparticles into base fluids will decrease the capacity and, thus, the cost of the storage medium. Researchers have shown keen interest in the use of molten salts and ionic liquid nanofluids for solar applications.[38,39] In a study,[40] SHC enhancement in ionic liquid nanofluids was suggested to be driven by the existing interfacial nano-layering occurring on the surface of nanoparticles. Rizvi *et al.*[41] tested the thermophysical properties of Li_2CO_3–Na_2CO_3 and Li_2CO_3–K_2CO_3, and their nanofluids. SHC of Li_2CO_3–Na_2CO_3 and Li_2CO_3–K_2CO_3 nanofluids (measured by DSC) showed SHC enhancements of 25% and 20% with respect to their molten salt base fluids, respectively. In another study,[42] molten salt nanofluids were synthesized by adding SiO_2 nanoparticles (1 wt%) into a binary mixture of $NaNO_3$–KNO_3, and its SHC was measured using DSC over a temperature range of 130–340 °C. SHC enhancement of 15% was observed; this increase was attributed to the formation of dendritic salt nanostructures. Paul *et al.*[43] studied the thermophysical properties of nanoparticle-enhanced ionic liquids where Al_2O_3 was dispersed in four different ionic liquids over the temperature range of 25–345 °C. Average SHC enhancements of 9%, 28%, and 62% were observed compared to base fluid for 0.5, 1.0, and 2.5 wt% of Al_2O_3, respectively.

Diamond nanoparticles have attracted attention due to their mechanical, thermal, and electrical properties.[44] Although scarcely, diamond nanofluids have been studied for their thermophysical properties like thermal conductivity and viscosity;[45–47] however, specific heat studies are considerably lacking. The addition of nanoparticles in fluids may cause an increase or decrease in the SHC of nanofluids. Inconsistencies in the results of SHC of nanofluids in literature necessitate the investigation of the fluid behavior in terms of SHC for different nanofluids. Diamond nanoparticles in thermal oil have not been subjected to investigation for specific heat. This study measures the specific heat of diamond/thermal oil (THO) nanofluids prepared by the two-step method (at nanoparticle concentrations 0.25–1.00 wt%) and are stabilized using a non-ionic surfactant, using DSC over a temperature range of 35–80 °C.

Materials and methods

Materials

High-purity (98.3%) diamond nanoparticles with an average size 3–10 nm are acquired from US Research Nanomaterials, Inc. (USA). Nanoparticles have a specific surface area (SSA) of 272 $m^2\ g^{-1}$, pore volume of 1.314 $cm^3\ g^{-1}$ and a spherical morphology. The resistivity of nanoparticles is $7.7 \times 10^7\ \Omega\ cm^{-1}$ and true density is 3.05–3.30 $g\ cm^{-3}$. The base fluid is highly refined oil (THO), Caltex Texatherm 32, consisting of 70–99 wt% hydrocarbons (C15–C50). Non-ionic sorbitane trioleate (Span 85) is used as a stabilizing agent, which is acquired from Sigma-Aldrich, Malaysia. The purity, morphology and structure of nanoparticles are verified by subjecting them to different characterization techniques such as electron microscopy, Fourier transform infrared spectroscopy (FTIR) and X-ray diffraction (XRD).

Nanofluid preparation and validity

Diamond nanofluids are prepared by the two-step method at nanodiamond loadings of 0.25, 0.50, 0.75, and 1.00 wt%. Span 85 (a non-ionic surfactant) is added as a stabilizer. Diamond nanoparticles and surfactant are in amounts of 1 wt% and 7 wt% of the nanofluid, respectively. The rest of the nanofluid *i.e.* 92-% comprises the base fluid, *i.e.*, thermal oil. Nanofluid concentration is generally depicted in terms of nanoparticle concentration. However, in this study, (*e.g.*) 1 wt% nanofluid corresponds to 1 wt% nanoparticle concentration, 7% Span 85, and 92% thermal oil.

Non-ionic surfactants have the advantage of being neutral, non-corrosive (which may otherwise damage equipment and pipelines) and are suitable with oils. The stability of nanofluids is visually analyzed when nanoparticles and surfactant are added to base fluid at varying concentrations. Diamond nanoparticles and Span 85 are added into THO and subjected to ultrasonication for 1 hour using probe-type 20 kHz ultrasonic homogenizer (Biologics Inc., 150 V/T) with ultrasonic parameters of 30% pulse and 70% power. A water bath (Hahnshin, HS 3005 N) is used to maintain room temperature.[48]

Equipment and sampling

Specific heat of the different concentrations of diamond/THO nanofluids is experimentally measured at varying temperatures using a differential scanning calorimeter (DSC), TA Instrument Q2000. The DSC is calibrated using sapphire as

standard material with known heat capacity to establish a baseline, in order to measure the absolute value of the sample. This calibration involved both temperature and SHC calibration. An empty aluminium hermetic sample pan (Tzero mass pan) is used to record the baseline heat flow before experiments. This step ensured that any instrument-related anomalies are subtracted from the subsequent SHC measurements. Aluminium-based lids are also used for sample encapsulation with the Tzero Pans.

One drop of the sample is added to the pan from the middle of the sample test tubes. These samples are freshly prepared and ultrasonicated to avoid any agglomeration impact on the heat capacity of nanofluids, and added to the standard aluminium hermetic pan using a dropper. The pan and lids, as well as the samples, are all weighed using the Mettler Toledo XP6 Microbalance, attached as an accessory to the DSC unit. The pans and lids are weighed to ensure that there are no significant differences in the masses of each pan/lid compared to the reference. The balance is also tared before the sample is added onto the pan for measurement of the sample size. This mass of the sample is input into the TA software. The values of the mass of the sample are added to the DSC software for further analysis. DSC is set at a constant heating rate of 10 °C min^{-1} for all nanofluid samples. The actual sampling weights of the nanofluids and pan/lids using the Mettler Toledo XP6 Microbalance are given in the Appendix (Table 2).

Validity of measurements

The specific heat capacity was measured using DSC three times to validate and ensure the accuracy of the SHC values obtained, reducing uncertainty in experimental results and making them more reliable. The mean values of SHC for three runs of the experiment over the temperature range 35–80 °C are given in Fig. 1. The error bars represent the standard deviation; it can be observed that the standard deviation increases with temperature. This can be attributed to the instability caused by natural convection and increase in Brownian motion at higher temperatures. The average standard deviation obtained is 0.015, with a relative standard deviation of 0.59.

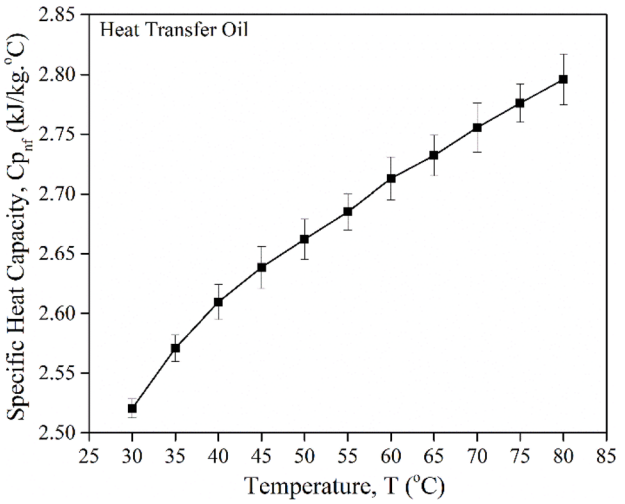

Fig. 1 Repetition of experimental specific heat capacity.

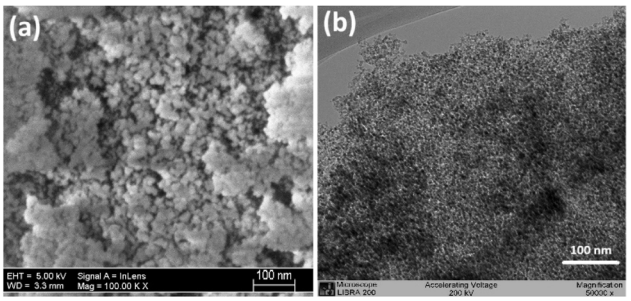

Fig. 2 Elemental microscopy of diamond nanoparticles: (a) SEM; (b) TEM.

Results and discussion

Nanoparticle characterization

The surface characterization of nanoparticles was performed using different techniques. Electron microscopy is used to study the size and morphology of the diamond nanoparticles. Fig. 2(a) and (b) shows the images of field emission scanning electron microscopy (FESEM) using Zeiss Supra 55 VP and transmission electron microscopy (TEM) using Zeiss Libra 200 kV, respectively. Some lumps are observed in these images, indicating an agglomerated state. The nanoparticle size and shape is observed to be consistent; the spherical shape of nanodiamond can be seen in the TEM image, confirming the information provided by the supplier. The X-ray diffraction (XRD) analysis (Bruker, D8 Advance) shows the crystalline characteristics of the nanoparticles, as presented in Fig. 3(a).

Two peaks are observed in the diffractogram at angles of 44.3° and 75.52°, exhibiting the diamond (111) and (220) phase

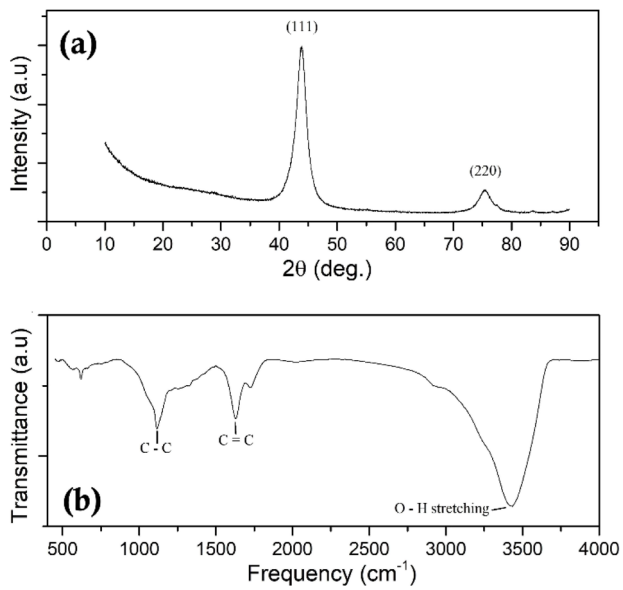

Fig. 3 Characterization of nanodiamonds *via*: (a) XRD; (b) FTIR.

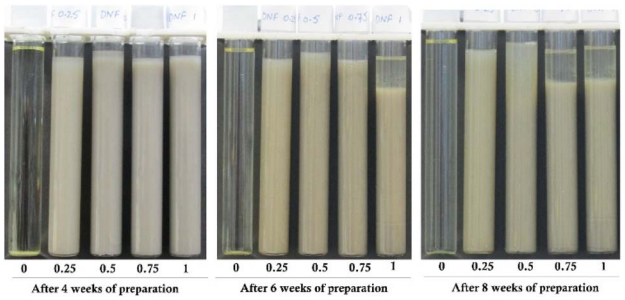

Fig. 4 Stability analysis of diamond/THO nanofluids at different concentrations.

nanostructure; the presence of no other peaks affirms the purity and uniform phase of nanodiamond.[49] Fig. 3(b) presents the FTIR spectrum of the diamond nanoparticles between frequencies 500–4000 cm^{-1}. Three major peaks represent O–H stretching (3300–3500 cm^{-1}), C=C (1535–1595 cm^{-1}), and C–C (around 1332 cm^{-1}).[50]

Stability analysis

It is important to investigate the stability of nanofluids for their appropriate use in applications. The stability of diamond/THO nanofluids was analyzed by observing the settling of nanoparticles at concentrations of 0.25, 0.50, 0.75 and 1.00 wt%, after 4,² 6 and 8 weeks of nanofluid preparation. Fig. 4 shows nanofluid samples at different concentrations. All concentrations were highly stable after 4 weeks with little to no settling observed. However, at 6 weeks, 1.00 wt% nanofluids started losing stability and significant settling was observed at 8 weeks for 0.5, 0.75 and 1.00 wt% nanofluids, in the ascending order. In other words, nanoparticle settling increases with increased particle concentration; the higher the concentration, the quicker the nanofluids lose their stability. 0.25 wt% nanofluids were stable even after 8 weeks. Overall, a fairly high stability is observed for this combination of nanofluids.

The dynamic light scattering (DLS) analysis was performed using the Malvern Zetasizer equipment to study the distribution of nanoparticles. The 0.25 wt% diamond/THO nanofluids were further diluted 20 times before analysis and three runs of DLS were done to ensure reliability of the analysis. Fig. 5 shows the particle size distributions with respect to volumetric percentage – the average diameter of the nanoparticle dispersions was 275 nm. The particle agglomerates in the nanofluids did not reach the micron size and were well within the nanoscale.

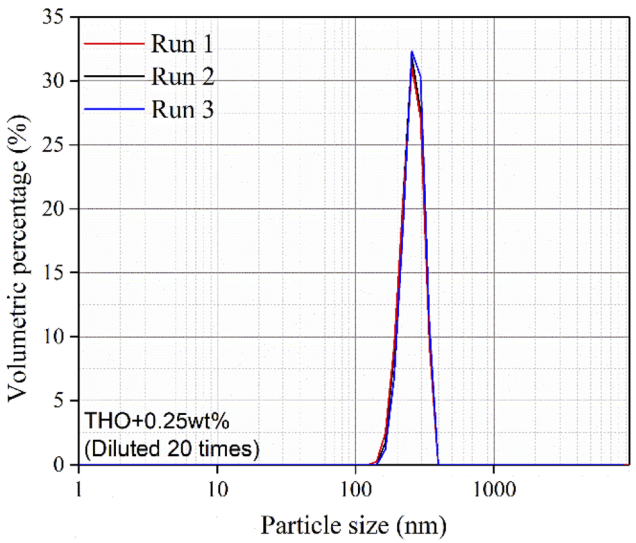

Fig. 5 DLS analysis of diamond/THO nanofluids.

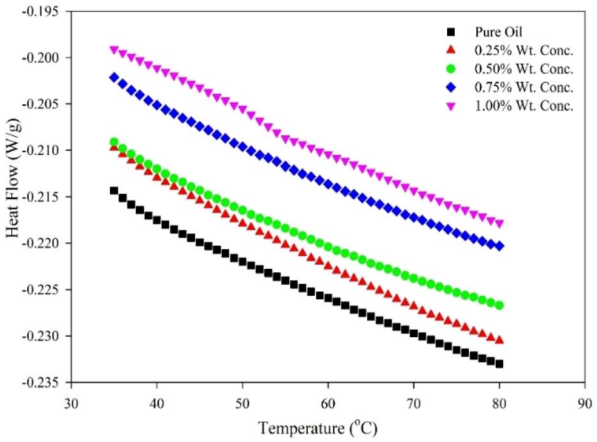

Fig. 6 Temperature *vs.* heat flow.

Thermograms of diamond-based nanofluids

Fig. 6 shows the thermograms of diamonds/THO nanofluids. No peak is observed as no phase change takes place between temperatures 35–80 °C. The heat flow of the nanofluids decreases with an increase in temperature, and increases as the nanoparticle concentration increases. The heat flow decreases from −0.2143 to −0.233 W g^{-1} for pure thermal oil, −0.2097 to −0.2305 W g^{-1} at 0.25 wt%, and from −0.1991 to −0.2178 W g^{-1}

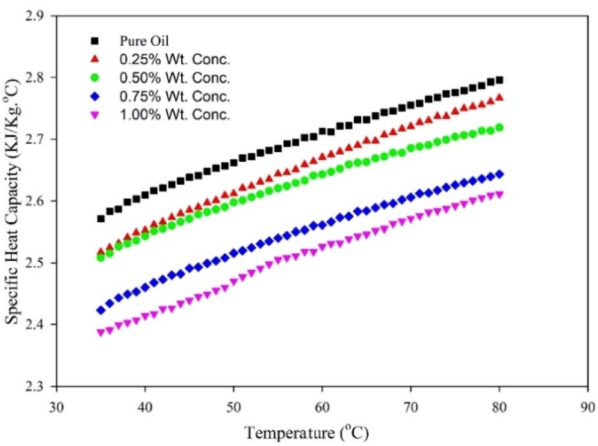

Fig. 7 Specific heat capacity of diamond/thermal oil nanofluids as a function of temperature.

at 1.00 wt% over the given temperature range. Maximum increase in heat flow *i.e.* 0.0167 W g^{-1} is observed at 45 °C from pure thermal oil to 1.00 wt% nanoparticle concentration.

Experimental heat capacity of diamond-based nanofluids

The SHC of thermal oil and diamond/THO nanofluids are measured for nanoparticle concentrations of 0.25, 0.50, 0.75 and 1.00 wt % in thermal oil over a temperature range of 35–80 °C. Fig. 7 illustrates the changes in SHC of thermal oil and nanofluids with different particle concentrations as a function of temperature. The SHC of the nanofluids decreased with an increase in nanoparticle concentration, the base fluid *i.e.* pure thermal oil has the highest SHC amongst all five samples, while SHC of both pure oil and diamond/THO nanofluids increased with increasing temperatures. The SHC of pure oil ranged from 2.57 to 2.79 kJ kg^{-1} $°C^{-1}$ over the given temperature range while the lowest SHC values obtained by 1.00 wt% nanoparticle concentration in base fluid were 2.38–2.61 kJ kg^{-1} $°C^{-1}$. Fig. 8 compares the SHC of pure oil with each of the four nanofluid samples in terms of percentage decrement. Reduction in SHC can be observed with increase in particle concentration at all temperatures. Maximum decrements of 2.32%, 2.91%, 6.12% and 8.25%, and lowest percentage reductions of 1.05%, 2.39%, 5.61% and 6.99% are obtained for 0.25, 0.50, 0.75 and 1.00% nanoparticle concentrations respectively.

Addition of nanoparticles into some base fluid may increase or decrease the SHC of the nanofluids depending on the type of nanoparticle and base fluid, and their individual thermophysical properties. The SHC of nanofluids tend to decrease if the nanoparticles have a lower SHC than the base fluid. Suspension of nanoparticles also changes the solid–liquid interfacial free energy. The larger specific surface area of the nanoparticles allows there to be a greater proportion of surface free energy in the system capacity, thus changing the SHC of nanofluids.[5] Nanofluids having a lower heat capacity are useful in applications where quick temperature changes are required, most often when dealing with low temperature range systems. Fluids can be tailored such that the addition of certain nanoparticles decreases its SHC.

Comparison with conventional models

There are two widely used models for specific heat in literature. Model 1, presented by Pak and Cho,[51] *i.e.* the ideal mixture model relates the SHC of the nanofluid ($C_{p,nf}$), to the SHC of base fluid ($C_{p,f}$) and nanoparticles ($C_{p,n}$), and volume fraction (φ), *i.e.* $C_{p,nf} = \varphi C_{p,n} + (1 - \varphi)C_{p,f}$. However, despite being a simple model, it is scarcely found to be justified where nanofluids are concerned. Model 2, proposed by Xuan and Roetzel[52] is based on the thermal equilibrium between the nanoparticles and the surrounding base fluid *i.e.* $C_{p,nf} = [\varphi(\rho C_p)_n + (1 - \varphi)(\rho C_p)_f]/[\varphi\rho_n + (1 - \varphi)\rho_f]$, where ρ_n and ρ_f are nanoparticle and fluid densities, respectively. Results of experimental studies on specific heat may or may not adhere to either or both of these models. Vallejo *et al.*[53] studied the thermophysical properties of α-SiC and β-SiC dispersed in propylene glycol + water (30 : 70) at 1 and 2 wt% of nanoparticles from 293.15–313.15 K. Both models showed good predictions for the measured experimental data of SHC, with average deviations of −0.07%, 0.16%, −0.03%, and 0.21% for the 1% α-SiC, 2% α-SiC, 1% β-SiC, and 2% β-SiC nanofluids, respectively for Model 1, and −0.3% and 0.1% for the 2% α-SiC and β-SiC nanofluids, respectively for Model 2. O'Hanley *et al.*[54] measured the SHC of water based silica, copper oxide and alumina nanofluids between nanoparticle concentrations of 5–50 wt%. While the results were in excellent agreement with Model 2, significant deviations were observed with the predictions of Model 1. Similarly, another study[17] investigated the SHC of titanium dioxide (TiO_2), aluminium oxide (Al_2O_3) and aluminium (Al) nanoparticles in deionized water, ethylene glycol (EG) and engine oil. The measured values showed good agreement with Model 2, with maximum deviations of 0.8%, 5.5%, and 7% for Al/EG, TiO_2/EG, and Al/engine oil nanofluids, respectively.

The SHC of diamond/THO nanofluids obtained in this study are not in agreement with either Model 1 or 2. As shown in Fig. 9, the SHC measured by DSC deviate significantly from the SHC evaluated from both these models, which tend to overestimate the SHC of these nanofluids. Deviation from both models increased with nanoparticle concentration and decreased with an increase in temperature. There is a maximum deviation of 7.45% and 8.63% at 35 °C from Model 1 and 2,

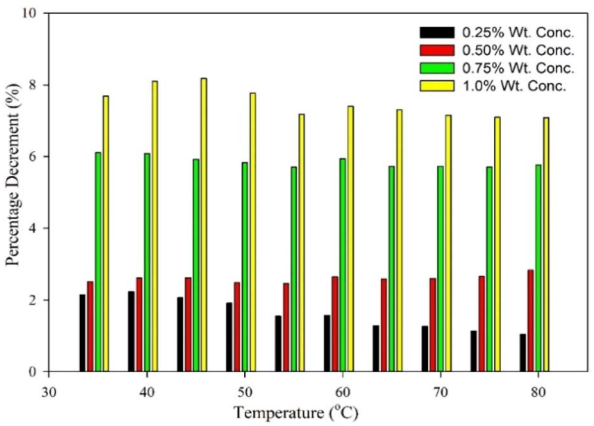

Fig. 8 Percentage decrement of the measured SHC for diamond/thermal oil nanofluids.

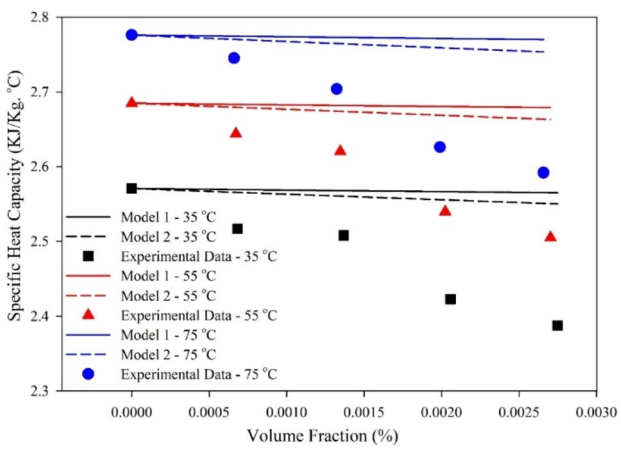

Fig. 9 Comparison of experimental SHC with Model 1 and 2.

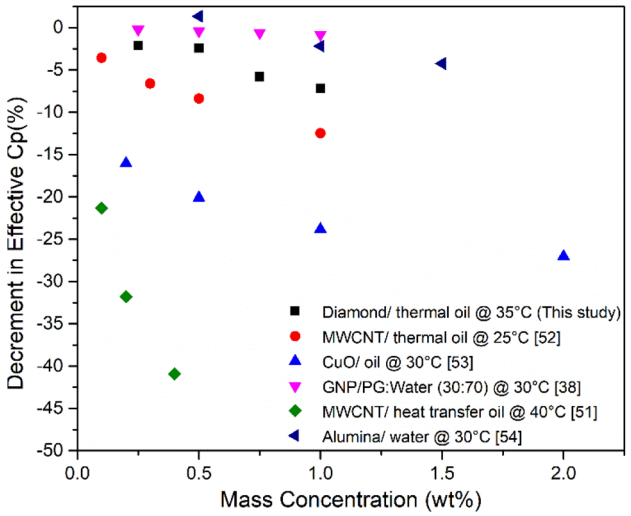

Fig. 10 Comparison of specific heat capacity decrement with other studies.

respectively. The limited application of Model 1 and 2 is also backed by several other studies in which these models were unable to validate their experimental data. Fakoor *et al.*[55] experimentally investigated the SHC of MWCNT/heat transfer oil, which did not validate these models. There was a maximum deviation of 40% from Model 1 for 0.4 wt% nanofluid at 40 °C, and that of 22% from Model 2 at 0.2 wt% at 70 °C. Similarly, these models overpredicted the SHC for other studies as well.[56,57] These models do not give accurate predictions of SHC because of their inability to take into consideration several factors like size effects and aggregation between nanoparticles, presence of functional group on nanoparticle surface, density of nanoparticles, temperature of the nanofluid, phonon transfer, Brownian motion and other phenomenon at nanoscale.

Comparison with existing experimental studies

Fig. 10 compares the decrease in SHC in this study to the decrement of other studies *i.e.* Ilyas *et al.*,[56] Saeedinia *et al.*,[57] Vallejo *et al.*,[35] Pakdaman *et al.*[55] and Teng *et al.*[58] Some studies show a more significant decrement than others; this study has a comparatively lesser decrement. However, it is to be noted that these SHC values are taken at a specific temperature (not over a range), and SHC decrements may vary with changes in temperatures.

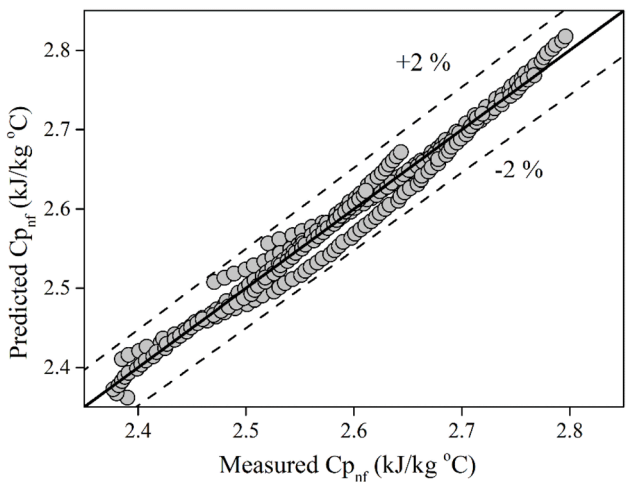

Fig. 11 Parity plot of the proposed multivariable correlation.

Proposed multivariable correlation

The proposed multivariable correlation for diamond/THO nanofluids, given in the equation below is a function of nanoparticle concentration (φ) and temperature (T). Fig. 11 shows the parity plot of this correlation, having an R^2 value (coefficient of determination) of 0.9635. It has an average absolute deviation (AAD) of 0.39729% and the sum of squared deviations (SSD) of 0.05489. The mean absolute error (MAE) is ±2%.

$$C_p = 2.399 - 0.1944\varphi + 0.005T$$

Conclusions

Nanoparticles added in some base fluid change its specific heat capacity (SHC). While there are several studies available on the thermal conductivity and viscosity of nanofluids, SHC requires more investigation to understand the fluid behavior of different nanofluids. In this study, the SHC of diamond/thermal oil nanofluids is measured by differential scanning calorimeter (DSC) over a temperature range of 35–80 °C for nanoparticle concentrations 0.25, 0.50, 0.75, and 1.00 wt%. The SHC of these nanofluids was observed to have decreased with nanoparticle concentration, while it increased with temperature, showing a maximum decrement of 8.25% at 1.00 wt%. The SHC values obtained significantly differed from the two classical models used to determine SHC. A multivariable correlation is proposed to determine SHC of diamond/thermal oil nanofluids in the temperature range 35–80 °C, which has an R^2 value of 0.9635 and MAE of ±2%.

Data availability

All the data is included in the manuscript.

Author contributions

Conceptualization, A. A., S. U. I., and M. A.; data curation, A. A., and S. U. I.; formal analysis, A. A., A. A., N. N., A. M., and M. A.; funding acquisition, A. A.; investigation, M. A., S. U. I. and A. A.; methodology, A. A., S. U. I., N. N., M. A., and A. A.; resources, S. U. I., and M. A.; supervision, S. U. I.; validation, A. A., A. A. and S. U. I.; visualization, N. N. and A. M.; writing – original draft, A. A., and N. N.; writing – review and editing, S. U. I. and A. A. All authors have read and agreed to the published version of the manuscript.

Conflicts of interest

The authors declare no conflicts of interest.

Appendix

Table 2 Sample size for the DSC testing using aluminium hermetic sample pan

		Pan mass (mg)	
Sample name	Sample size (mg)	Sample	Reference
Thermal oil	11.2530	53.374	53.108
0.25% nanofluid	13.6940	51.984	53.108
0.5% nanofluid	13.6190	53.333	53.108
0.75% nanofluid	15.5650	52.368	53.108
1.0% nanofluid	17.2750	53.083	53.108

Acknowledgements

The authors acknowledge the University of Jeddah, KSA, for technical and financial support. This work was funded by the University of Jeddah, Jeddah, Saudi Arabia, under grant no. (UJ-23-SRP-9).

Notes and references

1 M. Alsaady, T. C. Ray, S. U. Ilyas, A. Abdulrahman and R. Shamsuddin, Application of Hexagonal Boron Nitride Nanoparticles in Thermal Improvement of Oil-Based Nanofluids Stabilized With Non-Ionic Surfactant, *Proc ASME 2024 7th Int Conf Micro/Nanoscale Heat Mass Transfer MNHMT*, 2024, DOI: **10.1115/MNHMT2024-132797**.

2 S. U. Ilyas, M. Narahari and R. Pendyala, Rheological characteristics of ultrastable diamond-thermal oil nanofluids, *J. Mol. Liq.*, 2020, **309**, 113098, DOI: **10.1016/J.MOLLIQ.2020.113098**.

3 L. Godson, B. Raja, D. Mohan Lal and S. Wongwises, Enhancement of heat transfer using nanofluids-An overview, *Renewable Sustainable Energy Rev.*, 2010, **14**(2), 629–641, DOI: **10.1016/j.rser.2009.10.004**.

4 E. De Robertis, E. H. H. Cosme, R. S. Neves, A. Y. Kuznetsov, A. P. C. Campos, S. M. Landi, *et al.*, Application of the modulated temperature differential scanning calorimetry technique for the determination of the specific heat of copper nanofluids, *Appl. Therm. Eng.*, 2012, **41**, 10–17, DOI: **10.1016/j.applthermaleng.2012.01.003**.

5 I. M. Shahrul, I. M. Mahbubul, S. S. Khaleduzzaman, R. Saidur and M. F. M. Sabri, A comparative review on the specific heat of nanofluids for energy perspective, *Renewable Sustainable Energy Rev.*, 2014, **38**, 88–98, DOI: **10.1016/j.rser.2014.05.081**.

6 R. R. Souza, V. Faustino, I. M. Gonçalves, A. S. Moita, M. Bañobre-López and R. Lima, A Review of the Advances and Challenges in Measuring the Thermal Conductivity of Nanofluids, *Nanomaterials*, 2022, **12**(15), 2526, DOI: **10.3390/nano12152526**.

7 R. Lenin, P. A. Joy and C. Bera, A review of the recent progress on thermal conductivity of nanofluid, *J. Mol. Liq.*, 2021, **338**, 116929, DOI: **10.1016/j.molliq.2021.116929**.

8 H. Younes, M. Mao, S. M. Sohel Murshed, D. Lou, H. Hong and G. P. Peterson, Nanofluids: key parameters to enhance thermal conductivity and its applications, *Appl. Therm. Eng.*, 2022, **207**, 118202, DOI: **10.1016/j.applthermaleng.2022.118202**.

9 S. A. Ebrahim, E. Pradeep, S. Mukherjee and N. Ali, Rheological behavior of dilute graphene-water nanofluids using various surfactants: an experimental evaluation, *J. Mol. Liq.*, 2023, **370**, 120987, DOI: **10.1016/j.molliq.2022.120987**.

10 S. N. E. B. Nik, S. U. Ilyas, S. A. A. Taqvi, N. Noshad, R. Shamsuddin, S. L. S. Mun, *et al.*, Rheological Behavior Predictions of Non-Newtonian Nanofluids *via* Correlations and Artificial Neural Network for Thermal Applications, *Digit. Chem. Eng.*, 2024, 100170, DOI: **10.1016/j.dche.2024.100170**, **https://linkinghub.elsevier.com/retrieve/pii/S2772508124000322**.

11 J. Shelton, N. K. Saini and S. M. Hasan, Experimental study of the rheological behavior of TiO_2–Al_2O_3/mineral oil hybrid nanofluids, *J. Mol. Liq.*, 2023, **380**, 121688, DOI: **10.1016/j.molliq.2023.121688**.

12 H. Adun, I. Wole-Osho, E. C. Okonkwo, D. Kavaz and M. Dagbasi, A critical review of specific heat capacity of hybrid nanofluids for thermal energy applications, *J. Mol. Liq.*, 2021, **340**, 116890, DOI: **10.1016/j.molliq.2021.116890**.

13 A. Ali, H. Naseer, S. U. Ilyas, P. E. Phelan, R. Nasir, M. Alsaady, *et al.*, Thermal and Rheological Behavior of Hybrid Nanofluids Containing Diamond and Boron Nitride in Thermal Oil for Cooling Applications, *Arab. J. Sci. Eng.*, 2024, **49**(6), 7811–7828. Available from: **https://link.springer.com/article/10.1007/s13369-023-08467-4**.

14 S. Akilu, A. T. Baheta, K. V. Sharma and M. A. Said, Experimental determination of nanofluid specific heat with SiO2 nanoparticles in different base fluids, *AIP Conf. Proc.*, 2017, **1877**(1), 090001, DOI: **10.1063/1.4999896**.

15 D. Cabaleiro, C. Gracia-Fernández, J. L. Legido and L. Lugo, Specific heat of metal oxide nanofluids at high concentrations for heat transfer, *Int. J. Heat Mass Transf.*, 2015, **88**, 872–879, DOI: **10.1016/j.ijheatmasstransfer.2015.04.107**.

16 M. Vaka, M. Khalid and J. Paul, A review of different models, mechanisms, theories and parameters in tuning the specific heat capacity of nano-phase change materials, *J. Energy Storage*, 2023, **72**(PE), 108678, DOI: **10.1016/j.est.2023.108678**.

17 S. M. S. Murshed, Determination of effective specific heat of nanofluids, *J. Exp. Nanosci.*, 2011, **6**(5), 539–546, DOI: **10.1080/17458080.2010.498838**.

18 B. Ma, D. Shin and D. Banerjee, One-step synthesis of molten salt nanofluid for thermal energy storage application – a comprehensive analysis on thermophysical property,

corrosion behavior, and economic benefit, *J. Energy Storage*, 2021, **35**, 102278, DOI: 10.1016/j.est.2021.102278.

19 H. Riazi, T. Murphy, G. B. Webber, R. Atkin, S. S. M. Tehrani and R. A. Taylor, Specific heat control of nanofluids: A critical review, *Int. J. Therm. Sci.*, 2016, **107**, 25–38, DOI: 10.1016/j.ijthermalsci.2016.03.024.

20 M. Gamal, M. S. Radwan, I. G. Elgizawy and M. H. Shedid, Thermophysical characterization on water and ethylene glycol/water-based MgO and ZnO nanofluids at elevated temperatures: An experimental investigation, *J. Mol. Liq.*, 2023, **369**, 120867, DOI: 10.1016/j.molliq.2022.120867.

21 M. P. Shevelyova, Y. U. Paulechka, G. J. Kabo, A. V. Blokhin, A. G. Kabo and T. M. Gubarevich, Physicochemical properties of imidazolium-based ionic nanofluids: Density, heat capacity, and enthalpy of formation, *J. Phys. Chem. C*, 2013, **117**(9), 4782–4790, DOI: 10.1021/jp3059432.

22 E. I. Cherecheş, D. Bejan, C. Ibanescu, M. Danu and A. A. Minea, Nanocolloids based on PEG 400 with MgO nanoparticles: Experimental study on viscosity and specific heat, *Therm. Sci. Eng. Prog.*, 2023, **43**, 0–11, DOI: 10.1016/j.tsep.2023.101985.

23 K. Cwynar, J. Dziadosz, Ł. Scheller, E. Zorębski, R. Jędrysiak, A. Kolanowska, *et al.*, On isobaric heat capacity of ionanofluids with carbon nanotubes – An experimental study, *J. Mol. Liq.*, 2023, **387**, 122535, DOI: 10.1016/j.molliq.2023.122535.

24 H. Adun, D. Kavaz, I. Wole-Osho and M. Dagbasi, Synthesis of Fe_3O_4-Al_2O_3-ZnO/water ternary hybrid nanofluid: investigating the effects of temperature, volume concentration and mixture ratio on Specific heat capacity, and development of Hybrid machine learning for prediction, *J. Energy Storage*, 2021, **41**, 102947, DOI: 10.1016/j.est.2021.102947.

25 A. Hosseinghorbani, M. Mozaffarian and G. Pazuki, Application of graphene oxide IoNanofluid as a superior heat transfer fluid in concentrated solar power plants, *Int. Commun. Heat Mass Transf.*, 2020, **111**, 104450, DOI: 10.1016/j.icheatmasstransfer.2019.104450.

26 Z. Said, M. Ghodbane, L. S. Sundar, A. K. Tiwari, M. Sheikholeslami and B. Boumeddane, Heat transfer, entropy generation, economic and environmental analyses of linear fresnel reflector using novel rGO-Co_3O_4 hybrid nanofluids, *Renew. Energy*, 2021, **165**, 420–437, DOI: 10.1016/j.renene.2020.11.054.

27 I. Wole-Osho, E. C. Okonkwo, D. Kavaz and S. Abbasoglu, An experimental investigation into the effect of particle mixture ratio on specific heat capacity and dynamic viscosity of Al_2O_3–ZnO hybrid nanofluids, *Powder Technol.*, 2020, **363**, 699–716, DOI: 10.1016/j.powtec.2020.01.015.

28 H. Yarmand, S. Gharehkhani, S. F. S. Shirazi, M. Goodarzi, A. Amiri, W. S. Sarsam, *et al.*, Study of synthesis, stability and thermo-physical properties of graphene nanoplatelet/platinum hybrid nanofluid, *Int. Commun. Heat Mass Transf.*, 2016, **77**, 15–21, DOI: 10.1016/j.icheatmasstransfer.2016.07.010.

29 S. Akilu, A. T. Baheta, M. A. Mior, A. A. Minea and K. V. Sharma, Properties of glycerol and ethylene glycol mixture based SiO_2–CuO/C hybrid nanofluid for enhanced solar energy transport, *Sol. Energy Mater. Sol. Cells*, 2018, **179**, 118–128, DOI: 10.1016/j.solmat.2017.10.027.

30 T. C. Paul, A. K. M. M. Morshed, E. B. Fox and J. A. Khan, Thermal performance of Al_2O_3 Nanoparticle Enhanced Ionic Liquids (NEILs) for Concentrated Solar Power (CSP) applications, *Int. J. Heat Mass Transf.*, 2015, **85**, 585–594, DOI: 10.1016/j.ijheatmasstransfer.2015.01.071.

31 A. Ijam, R. Saidur, P. Ganesan and A. Moradi Golsheikh, Stability, thermo-physical properties, and electrical conductivity of graphene oxide-deionized water/ethylene glycol based nanofluid, *Int. J. Heat Mass Transf.*, 2015, **87**, 92–103, DOI: 10.1016/j.ijheatmasstransfer.2015.02.060.

32 R. Gómez-Villarejo, T. Aguilar, S. Hamze, P. Estellé and J. Navas, Experimental analysis of water-based nanofluids using boron nitride nanotubes with improved thermal properties, *J. Mol. Liq.*, 2019, **277**, 93–103, DOI: 10.1016/j.molliq.2018.12.093.

33 J. P. Vallejo, U. Calviño, I. Freire, J. Fernández-Seara and L. Lugo, Convective heat transfer in pipe flow for glycolated water-based carbon nanofluids. A thorough analysis, *J. Mol. Liq.*, 2020, **301**, 112370, DOI: 10.1016/j.molliq.2019.112370.

34 M. A. Marcos, J. Fal, J. P. Vallejo, G. Żyła and L. Lugo, Thermophysical, rheological and dielectric behaviour of stable carbon black dispersions in PEG200, *J. Mol. Liq.*, 2023, **391**, 1–10, DOI: 10.1016/j.molliq.2023.123216.

35 J. P. Vallejo, J. Perez-Tavarnier, D. Cabaleiro, J. Fernandez-Seara and L. Lugo. Heat Transfer Capability of Functionalized Graphene Nanoplatelet Dispersions in Propylene Glycol + Water (30:70 wt. %), *13th International Conference on Heat Transfer, Fluid Mechanics and Thermodynamics*. 2017, vol. 2, pp. 307–311.

36 W. Chen, C. Zou and X. Li, An investigation into the thermophysical and optical properties of SiC/ionic liquid nanofluid for direct absorption solar collector, *Sol. Energy Mater. Sol. Cells*, 2017, **163**, 157–163, DOI: 10.1016/j.solmat.2017.01.029.

37 G. Żyła, J. P. Vallejo, J. Fal and L. Lugo, Nanodiamonds – Ethylene Glycol nanofluids: Experimental investigation of fundamental physical properties, *Int. J. Heat Mass Transf.*, 2018, **121**, 1201–1213, DOI: 10.1016/j.ijheatmasstransfer.2018.01.073.

38 M. Chieruzzi, G. F. Cerritelli, A. Miliozzi and J. M. Kenny, Effect of nanoparticles on heat capacity of nanofluids based on molten salts as PCM for thermal energy storage, *Nanoscale Res. Lett.*, 2013, **8**(1), 1–9, DOI: 10.1186/1556-276X-8-448.

39 M. X. Ho and C. Pan, Experimental investigation of heat transfer performance of molten HITEC salt flow with alumina nanoparticles, *Int. J. Heat Mass Transf.*, 2017, **107**, 1094–1103, DOI: 10.1016/j.ijheatmasstransfer.2016.11.015.

40 K. Oster, C. Hardacre, J. Jacquemin, A. P. C. Ribeiro and A. Elsinawi, Understanding the heat capacity enhancement in ionic liquid-based nanofluids (ionanofluids), *J. Mol. Liq.*, 2018, **253**, 326–339, DOI: 10.1016/j.molliq.2018.01.025.

41 S. M. M. Rizvi and D. Shin, Specific heat capacity, viscosity, and thermal stability of carbonate-based molten salt nanofluids, *J. Energy Storage*, 2021, **43**, 103192, DOI: 10.1016/j.est.2021.103192.

42 F. B. El, S. M. M. Rizvi, Y. Nayfeh and D. Shin, Study of viscosity and heat capacity characteristics of molten salt nanofluids for thermal energy storage, *Sol. Energy Mater. Sol. Cells*, 2020, **210**, 110503, DOI: 10.1016/j.solmat.2020.110503.

43 T. C. Paul, A. K. M. M. Morshed, E. B. Fox and J. A. Khan, Enhanced thermophysical properties of NEILs as heat transfer fluids for solar thermal applications, *Appl. Therm. Eng.*, 2017, **110**, 1–9, DOI: 10.1016/j.applthermaleng.2016.08.004.

44 F. Mashali, E. M. Languri, J. Davidson, D. Kerns, W. Johnson, K. Nawaz, *et al.*, Thermo-physical properties of diamond nanofluids: a review, *Int. J. Heat Mass Transf.*, 2019, **129**, 1123–1135, DOI: 10.1016/j.ijheatmasstransfer.2018.10.033.

45 F. Mashali, E. Languri, G. Mirshekari, J. Davidson and D. Kerns, Nanodiamond nanofluid microstructural and thermo-electrical characterization, *Int. Commun. Heat Mass Transfer*, 2019, **101**, 82–88, DOI: 10.1016/j.icheatmasstransfer.2019.01.007.

46 L. S. Sundar, M. J. Hortiguela, M. K. Singh and A. C. M. Sousa, Thermal conductivity and viscosity of water based nanodiamond (ND) nanofluids: An experimental study, *Int. Commun. Heat Mass Transf.*, 2016, **76**, 245–255, DOI: 10.1016/j.icheatmasstransfer.2016.05.025.

47 A. Alshayji, A. Asadi and I. M. Alarifi, On the heat transfer effectiveness and pumping power assessment of a diamond-water nanofluid based on thermophysical properties: An experimental study, *Powder Technol.*, 2020, **373**, 397–410, DOI: 10.1016/j.powtec.2020.06.068.

48 S. U. Ilyas, M. Narahari and R. Pendyala, Rheological characteristics of ultrastable diamond-thermal oil nanofluids, *J. Mol. Liq.*, 2020, **309**, 113098, DOI: 10.1016/j.molliq.2020.113098.

49 S. Toermita, A. Burian, J. C. Dore, D. LeBolloch, M. Fujii and S. Hayashi, Diamond nanoparticles to carbon onions transformation: X-ray diffraction studies, *Carbon*, 2002, **40**(9), 1469–1474, DOI: 10.1016/S0008-6223(01)00311-6.

50 T. Petit and L. Puskar, FTIR spectroscopy of nanodiamonds: Methods and interpretation, *Diamond Relat. Mater.*, 2018, **89**, 52–66, DOI: 10.1016/j.diamond.2018.08.005.

51 B. C. Pak and Y. I. Cho, Hydrodynamic and Heat Transfer Study of Dispersed Fluids with Submicron Metallic Oxide Particles, *Int. J. Heat Mass Transf.*, 1998, **11**(2), 151–170. Available from: https://www.tandfonline.com/doi/abs/10.1080/08916159808946559.

52 Y. Xuan and W. Roetzel, Conceptions for heat transfer correlation of nanofluids, *Int. J. Heat Mass Transf.*, 2000, **43**(19), 3701–3707, DOI: 10.1016/S0017-9310(99)00369-5.

53 J. P. Vallejo, L. Febrero-Garrido, A. Cacabelos, A. González-Gil and L. Lugo, Influence of crystal structure on the thermophysical properties and figures-of-merit of propylene glycol: water-based SiC nanofluids, *Powder Technol.*, 2024, **433**, 119299, DOI: 10.1016/j.powtec.2023.119299.

54 H. O'Hanley, J. Buongiorno, T. McKrell and L. W. Hu, Measurement and model validation of nanofluid specific heat capacity with differential scanning calorimetry, *Adv. Mech. Eng.*, 2012, **4**, 181079, DOI: 10.1155/2012/181079.

55 M. Fakoor Pakdaman, M. A. Akhavan-Behabadi and P. Razi, An experimental investigation on thermo-physical properties and overall performance of MWCNT/heat transfer oil nanofluid flow inside vertical helically coiled tubes, *Exp. Therm. Fluid Sci.*, 2012, **40**, 103–111, DOI: 10.1016/j.expthermflusci.2012.02.005.

56 S. U. Ilyas, R. Pendyala and M. Narahari, Stability and thermal analysis of MWCNT-thermal oil-based nanofluids, *Colloids Surf., A*, 2017, **527**, 11–22, DOI: 10.1016/J.COLSURFA.2017.05.004.

57 M. Saeedinia, M. A. Akhavan-Behabadi and P. Razi, Thermal and rheological characteristics of CuO-Base oil nanofluid flow inside a circular tube, *Int. Commun. Heat Mass Transf.*, 2012, **39**(1), 152–159, DOI: 10.1016/j.icheatmasstransfer.2011.08.001.

58 T. P. Teng and Y. H. Hung, Estimation and experimental study of the density and specific heat for alumina nanofluid, *J. Exp. Nanosci.*, 2014, **9**(7), 707–718, DOI: 10.1080/17458080.2012.696219.